Antiviral Research 84 (2009) 185–193

Contents lists available at ScienceDirect

Antiviral Research

journal homepage: www.elsevier.com/locate/antiviral

Utility of RNAi-mediated *prnp* gene silencing in neuroblastoma cells permanently infected by prions: Potentials and limitations

Younghwan Kim[a,1], Boram Han[b,1], William Titlow[a], Charles E. Mays[a], Moosik Kwon[b], Chongsuk Ryou[a,*]

[a] *Sanders-Brown Center on Aging, Department of Microbiology, Immunology and Molecular Genetics, College of Medicine, University of Kentucky, 800 Rose St. HSRB-326, Lexington, KY 40536, USA*

[b] *Department of Genetic Engineering, Sungkyunkwan University, Suwon 440-746, Republic of Korea*

ARTICLE INFO

Article history:
Received 27 February 2009
Received in revised form 4 July 2009
Accepted 4 September 2009

Keywords:
Prion
PrP^{C}
PrP^{Sc}
RNAi
siRNA
shRNA

ABSTRACT

Prion diseases are incurable, transmissible neurodegenerative disorders in humans and animals. Because the disease-associated isoform of prion protein, PrP^{Sc}, is conformationally converted from cellular prion protein, PrP^{C}, knockdown of PrP^{C} expression by RNA interference (RNAi) implicates therapy for prion diseases. In this study, introduction of small interfering (si) and small hairpin (sh) RNAs targeting the prion protein gene (*prnp*) transcripts triggered specific gene silencing and reduced the PrP^{C} level in both prion-free and -infected neuroblastoma cell lines. Furthermore, this approach suppressed PrP^{Sc} formation and ultimately eliminated PrP^{Sc} from prion-infected cell lines. However, prolonged culture of cured cells resulted in reappearance of PrP^{Sc} in the cell population, presumably by de novo PrP^{Sc} formation from residual PrP^{C} uncontrolled by RNAi and PrP^{Sc} remained under the detection limit. Protein misfolding cyclic amplification assays further confirmed that lysate of cured cells was sufficient to support PrP^{Sc} propagation. Our data not only suggest a potential treatment option but also implicate a caveat for using an RNAi approach for prion diseases. These findings provide critical information required to advance RNAi-based prevention and therapy for prion diseases of humans and animals.

1. Introduction

RNA interference (RNAi) is a cellular mechanism by which post-transcriptional modification of a gene transcript can initiate the gene silencing process in cells (Hannon, 2002). RNAi was found to participate in cellular defense mechanisms against incoming foreign/parasitic genetic materials or abnormal endogenous mRNA (Schmidt, 2005). This cellular machinery has been known to regulate developmental stages of organisms (Sontheimer and Carthew, 2005). In laboratory experiments, introduction of exogenously provided small interfering (si) RNA to a cell led to degradation of specific mRNA homologous to the sequences of siRNAs. Compared to siRNA, small hairpin (sh) RNA offers advantages in silencing longevity as well as delivery options (Paddison et al., 2004). Application of RNAi is thus a means by which specific gene(s) of interest can be turned off without manipulating the genomic DNA. In fact, numerous studies have shown that many diseases can be approached by RNAi to achieve a therapeutic goal (Campochiaro, 2006; Davidson and Boudreau, 2007; Grimm and Kay, 2007; Pai et al., 2006).

Prion diseases including Creutzfeldt–Jakob disease in humans, scrapie in sheep, and bovine spongiform encephalopathy in cattle are transmissible, fatal neurodegenerative disorders (Prusiner, 1998). These diseases are pathologically characterized by neuronal cell loss, vacuolation, spongiform degeneration, gliosis, and accumulation of scrapie-associated prion protein (PrP^{Sc}) in the brain (Prusiner, 1998). The cause of these diseases is a proteinaceous pathogen termed the prion (Prusiner, 1982). PrP^{Sc}, a misfolded isoform of cellular prion protein (PrP^{C}), is the principal, and possibly the sole, constituent of this transmissible agent (Prusiner, 1982). For prion propagation, PrP^{Sc} serves as a template promoting the conformational conversion of endogenous PrP^{C} to PrP^{Sc} at the post-translational level (Prusiner, 1998). Thus, lack of PrP^{C} expression results in no transmission of disease in the animals (Bueler et al., 1993; Sailer et al., 1994), suggesting that PrP^{C} is a critical prerequisite for prion propagation and pathogenesis.

Although prion diseases potentially threaten public health (Belay and Schonberger, 2005), no therapy for the diseases is currently available. RNAi of PrP^{C} has been considered as a therapeutic approach because knockdown of PrP^{C} expression could result in deprivation of substrate for PrP^{Sc} formation and ultimately pre-

* Corresponding author. Tel.: +1 859 257 4016; fax: +1 859 257 8382.
E-mail address: cryou2@email.uky.edu (C. Ryou).
[1] These authors contributed equally to this work.

0166-3542/$ – see front matter © 2009 Elsevier B.V. All rights reserved.
doi:10.1016/j.antiviral.2009.09.002

Table 1
Duplex RNA sequences for mouse *prnp*-specific siRNA.

siRNA	Duplex RNA sequences	Target region in mouse *prnp* mRNA (nt)
siRNA-PrPT1	5′- CUGGAUAACAGAGAGACAA (dTdT)-3′ 3′-(dTdT) GACCUAUUGUCUCUCUGUU -5′	1712–1730
siRNA-PrPT2	5′- AACAUGUACCGCUACCCUA (dTdT)-3′ 3′-(dTdT) UUGUACAUGGCGAUGGGAU -5′	609–627
siRNA-PrPT3	5′- ACUUCACCGAGACCGAUGU (dTdT)-3′ 3′-(dTdT) UGAAGUGGCUCUGGCUACA -5′	742–760
Scrambled RNA	5′- CCUACGCCACCAAUUUCGU (dTdT)-3′ 3′-(dTdT) GGAUGCGGUGGUUAAAGCA -5′	

Target regions of each siRNA are indicated on the basis of nucleotide (nt) numbering shown in the mouse *prnp* mRNA (NM 011170). siRNA-PrPT denotes siRNA targeting *prnp* mRNA.

vent transmission of diseases. Feasibility of PrP^C knockdown by RNAi was suggested in earlier investigations (Daude et al., 2003; Tilly et al., 2003). Other studies reported improved specificity of siRNA (Ohnishi et al., 2008) and expression efficiency of shRNA targeting *prnp* (Sutou et al., 2007). Although their disease resistance was not assessed, murine and bovine transgenic models expressing significantly reduced PrP^C levels were developed by utilizing RNAi (Gallozzi et al., 2008; Golding et al., 2006). Recently, lentiviral vector-mediated RNAi was shown to be effective in prolonging survival of prion-infected mice (Pfeifer et al., 2006; White et al., 2008). Despite the advent of RNAi application to prion diseases, this approach has not proved to cure the disease. Although the onset of disease was delayed, all animals treated with RNAi against PrP^C eventually died of prion disease (Pfeifer et al., 2006; White et al., 2008). Why this would be the case, even with the active RNAi against PrP^C, is not clear. To estimate effectiveness of RNAi approach in treating prion diseases, we studied knockdown of PrP^C expression and elimination of PrP^{Sc} in a cell culture model of prion diseases. Here, we describe the parallel lines of evidence implicating both positive and negative aspects of RNAi approach as a treatment for prion diseases.

2. Materials and methods

2.1. siRNA and shRNA

The Turbo si-Designer (Bioneer, Daejeon, Korea) was utilized to identify the siRNA regions in mouse *prnp* mRNA sequences. Among several, three regions showing the highest "likelihood score" for gene silencing were chosen, and the scrambled sequence was determined. These duplex siRNAs and scrambled RNAs were purchased from Bioneer and shown in Table 1. Based on the guidelines described in an earlier study (Paddison et al., 2002), DNA fragments for shRNA composed of the siRNA region, its complementary sequences, hairpin loop sequences and 3′ terminal uridine tract were synthesized (Bioneer) (Fig. 2A). These fragments were cloned at the multicloning sites in a shRNA expression vector, *pSilencer*™ 2.1 U6 hygro vector (Ambion, Austin, TX) after digestion with BamH I and Hind III restriction enzymes. The shRNA and its scrambled sequences are shown in Fig. 2A. The secondary structure was predicted by a publically available application (RNAfold web server,[2] Institute for Theoretical Chemistry, University of Vienna, Austria). The DNA sequences of resultant recombinant plasmid constructs were confirmed by sequence determination (Macrogen, Seoul, Korea).

[2] The URL of the RNAfold server: http://rna.tbi.univie.ac.at/cgi-bin/RNAfold.cgi.

2.2. Cell culture, transfection and treatment with compounds

N2a (ATCC CCL-131) and ScN2a (scrapie-infected N2a) (Scott et al., 1988) neuroblastoma cells were cultured as described elsewhere (Mays et al., 2008). Cells were maintained in Dulbecco's Modified Eagle's Medium (high glucose; Invitrogen, Carlsbad, CA) containing 10% inactivated fetal bovine serum, 1% penicillin–streptomycin, 1% glutamax with 5% CO_2 at 37 °C. According to the manufacturer's instructions, 2×10^5 cells (per well) in the 12-well cell culture plate (Corning, Corning, NY) were transfected with duplex siRNAs (0–400 nM) using Lipofectamine 2000 (Invitrogen) and recombinant plasmids (0–2 μg) expressing shRNA using Lipofectamin (Invitrogen). Five micrograms of pPrP3F4, the plasmid expressing 3F4 tagged PrP (Scott et al., 1992), were also used for a set of transfection studies where indicated. For transient transfection, cells were harvested in 48 h post-transfection. For stable transfection, cells were further cultured for 3 weeks in the presence of 300 μg/ml hygromycin (Sigma–Aldrich, St. Louis, MO). Individual clones of stable transfectants and the mixed population of the clones were maintained for additional 40 days. Treatment of ScN2a cells with polyamidoamine generation 4.0 (PAMAM G4.0, Sigma–Aldrich) and quinacrine (Sigma–Aldrich) was carried out as described previously (Ryou et al., 2003; Supattapone et al., 1999). Treatment lasted for 6 days in the presence of 0.1 μM PAMAM G4.0 and 0.6 μM quinacrine.

2.3. RNA isolation and RT-PCR

RNA preparation and RT-PCR were performed as described previously (Kim et al., 2009). RNA isolation from transfected cells using Trizol (Invitrogen) solution was performed according to the manufacturer's instructions. The concentration and purity of the isolated total RNA were measured by spectrometer (DU530, Beckman-Coulter, Fullerton, CA). cDNA was synthesized with 2 μg of total RNA using TaqMan Reverse Transcription Reagents kit (Applied Biosystems, Foster City, CA). For the conventional RT-PCR, 2 μl of cDNA and 25 pmol of each gene specific primer were mixed in 25 μl of PCR Supermix (Invitrogen). Sequences for *prnp*- and *β-actin*-specific primer pairs used in PCR are summarized in Table 2. PCR was performed in an Eppendorf MasterCycler under the following conditions: initial denaturation at 94 °C for 3 min, 30 cycles of

Table 2
PCR primers specific for mouse *prnp* and *β-actin* genes.

Primers	Sequences
moPrP F	5′-ATGGCGAACCTTGGCTAC-3′
moPrP R	5′-TCCCACGATCAGGAAGAT-3′
Actin F	5′-GATATCGCTGCGCTGGTCGTC-3′
Actin R	5′-CATCGTACTCCTGCTTGCTGAT-3′

denaturation at 94 °C for 60 s, annealing at 56 °C for 60 s, and amplification at 72 °C for 60 s. Amplicons were analyzed by agarose gel (1%) electrophoresis.

The mRNA levels of *prnp* and *β-actin* genes were measured by real time quantitative RT-PCR (qRT-PCR) using a Roche LightCycler (Roche, Basel, Switzerland). Analyses were conducted in triplicate tubes RT-PCR in the absence of reverse transcriptase was performed for each sample to rule out genomic DNA contamination. The PCR primers shown in Table 2 were purchased from Invitrogen. One microliter of cDNA and 20 pmol of each primer were used in a 20 μl reaction mixture using LightCycler FastStart DNA Master SYBR Green I (Roche). The thermal cycling consisted of polymerase activation at 95 °C for 10 min, followed by 45 cycles of denaturation at 95 °C for 10 s, annealing at 56 °C for 10 s, and extension at 72 °C for 20 s (*β-actin*) and 40 s (*prnp*). The relative expression of the *prnp* gene in each sample was normalized to the *β-actin* transcript level. The cycle threshold (C_T) value for *prnp* and *β-actin* transcripts was determined. Difference of C_T values (ΔC_T) was calculated by (1):

$$\Delta C_T = (C_T \text{ of } prnp \text{ mRNA}) - (C_T \text{ of } \beta - actin \text{ mRNA}) \quad (1)$$

The relative fold difference in gene expression was calculated by the $2^{-\Delta\Delta C_T}$ method (2) and (3) (Livak and Schmittgen, 2001).

$$\Delta\Delta C_T = (\Delta C_T \text{ of targeted RNAi-treated sample}) - (\Delta C_T \text{ of negative control RNAi-treated sample}) \quad (2)$$

$$\text{fold change} = 2^{-\Delta\Delta C_T} \quad (3)$$

Percent knockdown of target mRNA was assessed by (4):

$$\%\,\text{knockdown} = 100 \times [1 - (\text{fold change})] \quad (4)$$

2.4. Western blotting

Cell lysate was prepared in lysis buffer (20 mM Tris, pH 8.0, 140 mM NaCl, 0.5% deoxycholate, 0.5% NP-40). Protein contents were measured by BCA protein assay kit (Pierce, Rockford, IL). To detect PrP^C, ~10–40 μg of lysate was directly analyzed by SDS-PAGE followed by Western blotting. To detect PrP^{Sc}, ~1 mg of cell lysate was treated with 20 μg/ml proteinase K (PK) (Invitrogen) for 1 h at 37 °C. Following PK inactivation by adding phenylmethylsufonylfluoride to the final concentration of 2 mM, the lysate was ultracentrifuged at 100,000 × *g* for 1 h at 4 °C in a bench top ultracentrifuge (TLX-50, Beckman). Samples were separated in 12% SDS-PAGE gels and transferred to PVDF membrane (Immobilon-FL, Millipore, Billerica, MA). PrP^C and PrP^{Sc} were detected by incubation with monoclononal anti-PrP antibodies, 6H4 (Prionics, Zurich, Switzerland) or 3F4 (Signet Laboratory, Boston, MA). β-Actin was detected by monoclonal anti-β-actin antibody ACTN05 (Neomark, Oviedo, FL). The peroxidase-conjugated anti-mouse IgG secondary antibody and an enhanced chemiluminescent substrate (ECL plus, Amersham Pharmacia, Piscataway, NJ) were used for signal development. Doc-It Image Analysis Software (UVP, Upland, CA) was used for densitometry analysis.

2.5. Protein misfolding cyclic amplification (PMCA)

PMCA, an in vitro assay to amplify a small amount of PrP^{Sc} by accelerating conformational conversion of PrP^C, was conducted according to methods described elsewhere (Castilla et al., 2005; Saborio et al., 2001). Lysate of N2a, ScN2a, and cured ScN2a cells in a 100-mm culture dish was prepared in 1 ml of phosphate-buffered saline (PBS) by repeated passing through 16–21 gauge needles. Ten percent brain homogenate of 6-week-old healthy Tg4112 mice (a gift from Dr. Glenn Telling, University of Kentucky) was prepared in PBS containing protease inhibitor cocktail (Roche), 1% Triton X-100, and 4 mM EDTA by the same method. Tg4112 mice express PrP^C about 4–5 times more than wild type FVB mice (Telling, unpublished data). Cell lysate was diluted 3-, 9- and 27-fold in 0.1 ml of brain homogenate of Tg4112 mice. PrP^{Sc} amplification was performed by 95 cycles of sonication and incubation at 37 °C in the system equipped with Misonix Sonicator 3000 and Fisher Isotemp water bath. PMCA samples were halved and digested with 100 μg/ml PK (Roche) for 1 h at 37 °C. The level of PrP^{Sc} formed by PMCA was measured by Western blotting.

3. Results

3.1. Silencing expression of prnp gene transcripts and PrP^C by duplex siRNAs

To test down-regulation of PrP^C expression by siRNAs, we transfected N2a cells with three different duplex siRNAs (Table 1) exhibiting the best likelihood of gene silencing from in silico assessment, and analyzed the effect in 48 h post-transfection. Various amounts (0–400 nM) of each duplex siRNAs were transiently delivered. Cells transfected with 300–400 nM of duplex siRNAs demonstrated cell death at 24 h post-transfection (data not shown). However, those transfected with 100 nM or less did not show any signs of cytotoxicity under microscopic evaluation and protein assay using BCA reagents (Pierce). Thus, we conducted our following studies using ≤100 nM of duplex siRNAs.

In the qRT-PCR measurement of *prnp* mRNA abundance, transfection with three different duplex siRNAs showed effective down-regulation of *prnp* gene expression in a dose-responsive manner (Fig. 1A). siRNA-PrPT2 exhibited the most potent *prnp* gene silencing activity: 98–99% of *prnp* mRNA was knocked down by siRNA-PrPT2 compared to controls. Depending on the concentrations (50–100 nM), siRNA-PrPT1 and siRNA-PrPT3 knocked down 70.5–97.5% and 7.3–70.9% of *prnp* mRNA, respectively. However, scrambled siRNA containing sequences unrelated to any known gene was unable to interfere with expression of *prnp* gene transcripts.

Similarly, at the protein level, transfection of N2a cells with duplex siRNAs resulted in diminished PrP^C, whereas the level of β-actin remained steady (Fig. 1B). Both siRNA-PrPT1 and 2 abolished expression of PrP^C considerably at 50 nM and almost completely at 100 nM. Although dose-responsive, siRNA-PrPT3 was not as efficient as the other two siRNAs, decreasing the PrP^C levels only by 20–40% when estimated by densitometry. Scrambled RNA did not affect expression of PrP^C. Together with studies at the RNA level, these data suggest that siRNA-PrPT2 is the most effective siRNA targeting *prnp* among those tested.

3.2. Knockdown of prnp messages and its protein product using shRNA

Since siRNAs exert their effects temporarily during the first few days after transfection, constitutive expression of shRNA in cells is necessary to develop therapy or generate an animal model resistant to prion diseases. Feasibility of the shRNA strategy in knocking down *prnp* messages and PrP^C was assessed in N2a cells. For this study, RNA sequences of scrambled siRNA and siRNA-PrPT2 that exhibited the most potent targeting activity in our studies (Fig. 1) were chosen to generate plasmid constructs. Double-stranded DNAs encoding shRNAs of scrambled and target sequences were cloned in a mammalian small RNA expression

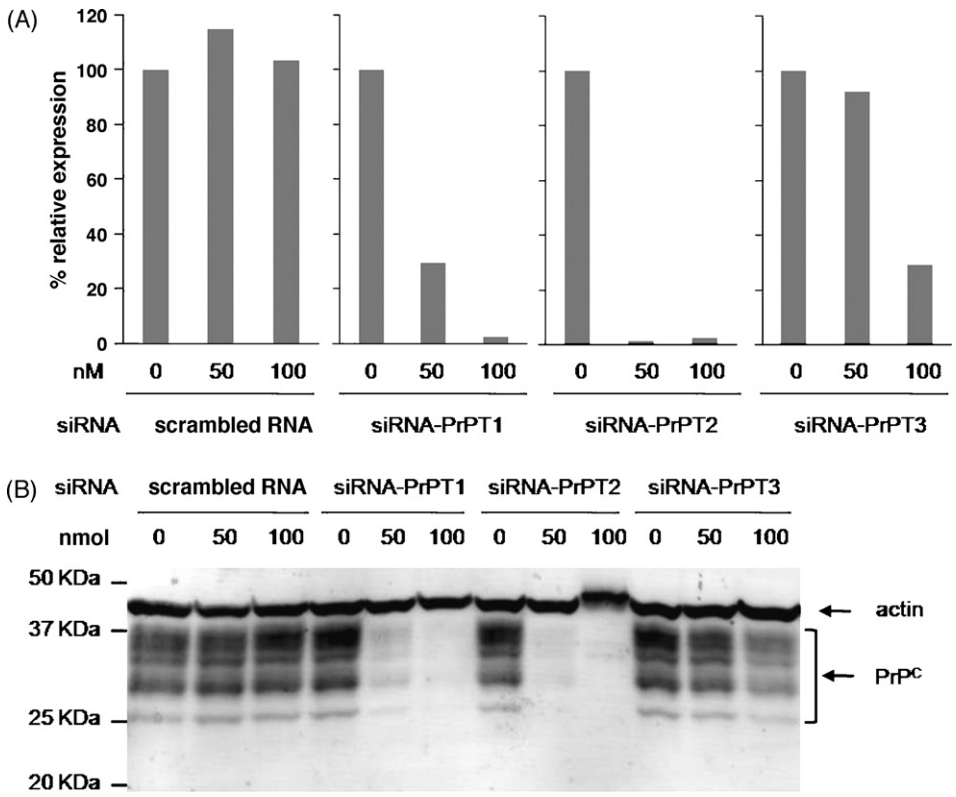

Fig. 1. Knockdown of *prnp* mRNA and PrP^C by siRNAs. N2a cells were transfected with siRNAs targeting *prnp* (siRNA-PrPT1, siRNA-PrPT2, and siRNA-PrPT3) and scrambled RNA sequences (0–100 nM). The transfectants were analyzed 48 h post-transfection. (A) The relative expression of *prnp* mRNA measured by qRT-PCR. (B) Western blotting of PrP^C and β-actin using monoclonal anti-PrP (6H4) and anti-β-actin (ACTN05) antibodies.

plasmid, pSilencer2.1 U6 hygro, containing human U6 RNA pol III promoter. The resultant plasmids expressing shRNA were termed pShRNA-PrPS and pShRNA-PrPT. The predicted secondary structures of shRNA targeting *prnp* and scrambled shRNA are shown in Fig. 2A.

Knockdown of *prnp* gene expression was estimated by transient transfection with pShRNA-PrPT. Conventional RT-PCR showed that the *prnp* mRNA levels were substantially reduced in cells transfected with pShRNA-PrPT, but unchanged in those transfected with pShRNA-PrPS compared to mock transfectants (Fig. 2B). *β-Actin* expression remained the same independent of shRNA expression (Fig. 2B). In qRT-PCR analysis, 81–89% of *prnp* mRNA was reduced in N2a cells transfected with pShRNA-PrPT compared to the mock and pShRNA-PrPS-transfected controls (Fig. 2C). These data suggest that expression of shRNA silenced expression of *prnp* messages in neuroblastoma cells.

In Western blot analysis, the decrease of PrP^C in N2a cells was also dependent on the expression of pShRNA-PrPT. The PrP^C levels were reduced by transfection with the increased amounts of pShRNA-PrPT, whereas introduction of pShRNA-PrPS did not interfere with expression of PrP^C (Fig. 2D). Densitometry analysis showed that ~97% of PrP^C expression was knocked down in N2a cells transfected with 2 μg of pShRNA-PrPT. These results support that expression of shRNA suppressed PrP^C expression.

3.3. RNAi-mediated inhibition of PrP^{Sc} formation in prion-infected neuroblastoma cells

To test whether expression of shRNA targeting *prnp* inhibits PrP^{Sc} formation, ScN2a cells were transfected with pShRNA-PrPT. Transient transfection substantially reduced the levels of PrP^C in these cells (Fig. 3A). This subsequently resulted in a partial (~50%) decrease, but not the complete elimination, of PrP^{Sc} (Fig. 3A). In the mock and control transfection with pShRNA-PrPS, the levels of PrP^C, PrP^{Sc} and β-actin remained unchanged.

The fate of the partially decreased but remaining PrP^{Sc} in transient transfectants with pShRNA-PrPT was monitored over time to clarify if incomplete PrP^{Sc} clearance was due to insufficient time for shRNA to be expressed. Residual PrP^{Sc} levels at 48 h post-transfection remained reduced even after 120 h, and did not disappear over the time (Fig. 3B). PrP^C was maintained at the significantly reduced levels during this period, indicating that expression of shRNA targeting *prnp* is functional in suppressing PrP^C expression and keeping PrP^C levels low for a few days. Our results indicate that the level of newly generated PrP^{Sc} would be minimal when shRNA is expressed, while most of the remaining PrP^{Sc} in the cells represents the PrP^{Sc} accumulated before RNAi. This suggests that RNAi prevents PrP^{Sc} formation, but is incapable of eliminating pre-accumulated PrP^{Sc}.

To confirm the interference with de novo generation of PrP^{Sc} by expression of shRNA targeting *prnp*, ScN2a cells were co-transfected with pShRNA-PrPT and pPrP3F4 expressing the epitope-tagged PrP^C. In this system, nascent expression of PrP^C and formation of PrP^{Sc} can be monitored from 3F4 epitope-tagged PrP^C, termed PrP^C3F4. This protein is a chimeric mouse prion protein (PrP) with a unique epitope of Syrian hamster (SHa) PrP (Scott et al., 1992) that is capable of being converted into a scrapie form as well as being discriminated from endogenous PrP^C and PrP^{Sc} when expressed in ScN2a cells. Monoclonal antibody 3F4 recognizes the unique epitope of SHa PrP included in PrP3F4. In Western blot analysis with the anti-PrP antibody 3F4, expression of PrP^C3F4 and formation of PrP^{Sc}3F4 were completely inhibited by expression of pShRNA-PrPT (Fig. 3C). In contrast, expression and formation

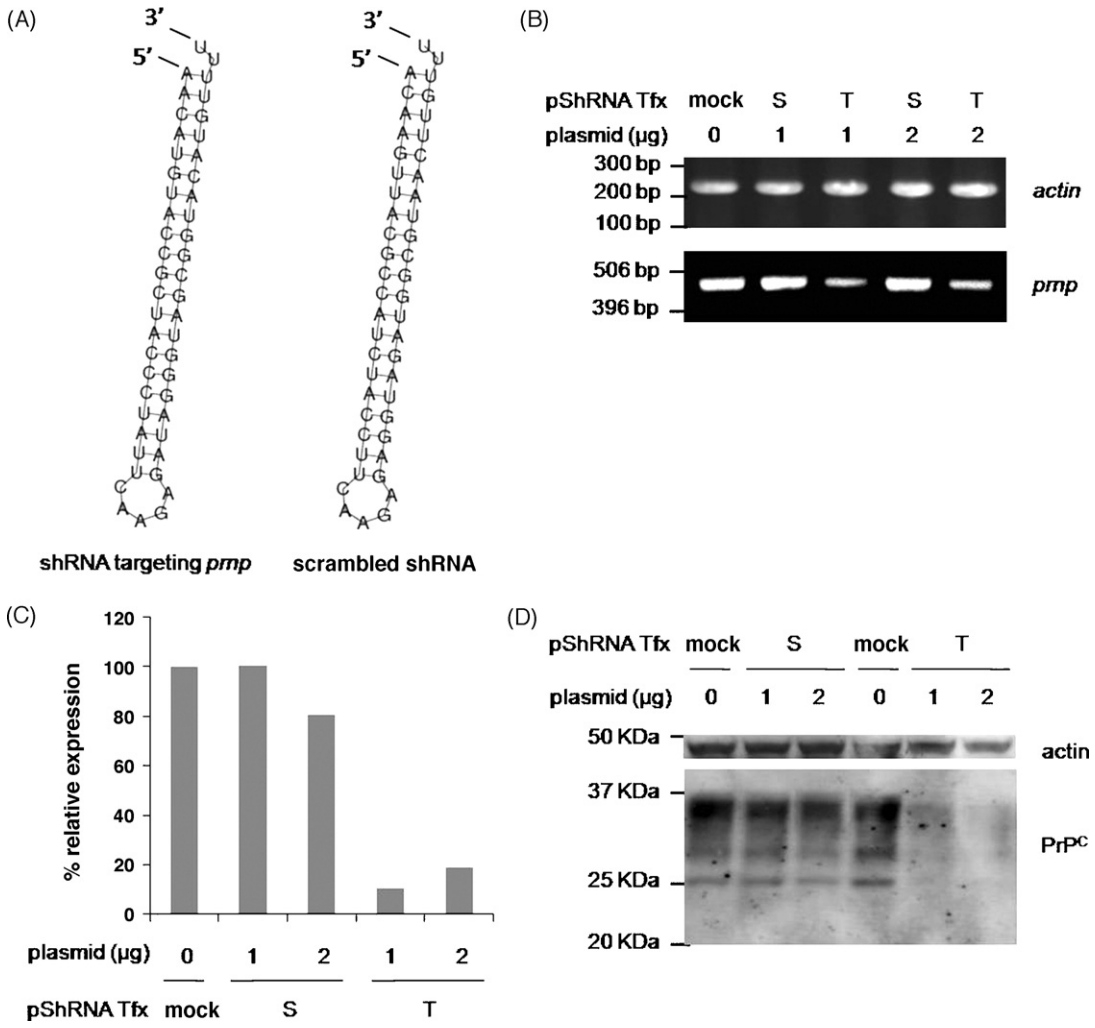

Fig. 2. Decrease of *prnp* mRNA and PrP^C by transient expression of shRNA. N2a cells were transfected with two plasmid constructs; pShRNA-PrPT (T) containing target sequences for *prnp* and pShRNA-PrPS (S) containing scrambled sequences. The transfectants were analyzed 48 h post-transfection. The mock transfection was performed with no plasmid DNAs. (A) The predicted secondary structure of shRNA targeting *prnp* (left) and scrambled shRNA (right). (B) Agarose gel electrophoresis of conventional RT-PCR products. The primer pairs for *prnp* and *β-actin* genes were designed to generate the amplicons of 426 bp (*prnp*) and 257 bp (*β-actin*). The 100 bp and 1 kbp ladder DNA markers (Invitrogen) were utilized as standards. (C) Relative abundance of *prnp* mRNA measured by qRT-PCR. Expression of *β-actin* transcripts was utilized to normalize *prnp* gene transcripts. (D) Western blotting of PrP^C and β-actin using monoclonal anti-PrP (6H4) and anti-β-actin (ACTN05) antibodies. Tfx: transfection.

of both isoforms of PrP3F4 were not affected in the mock and pShRNA-PrPS-transfected controls (Fig. 3C). When the same samples were analyzed by the anti-mouse PrP antibody, 6H4, which detects both endogenous PrP and PrP3F4, the profiles of endogenous PrP^C expression and PrP^{Sc} accumulation were identical to those previously shown in Fig. 3A. These results reassure that RNAi inhibits PrP^{Sc} formation via knockdown of PrP^C, while it is insufficient to eliminate pre-formed PrP^{Sc}.

To ascertain the effect of constitutive expression of shRNA in PrP^{Sc} accumulation, ScN2a cells were stably transfected with pShRNA-PrPT and selected in the presence of hygromycin. The mixed population (Fig. 3D) and randomly chosen individual clones (Fig. 3E) of stable transfectants exhibited substantial reduction of PrP^C levels as well as absolute elimination of PrP^{Sc} in Western blots. The levels of PrP^C expression and PrP^{Sc} accumulation were not changed obviously in the pShRNA-PrPS-transfected controls and were comparable to those in untranfected ScN2a cells (Fig. 3D). Individual clones (T#7, 8, and 9) stably transfected with pShRNA-PrPT remained free of PrP^{Sc} and appeared to express different levels of PrP^C, which were always lower than pShRNA-PrPS-transfected controls (Fig. 3E). These data suggest that constitutive expression of shRNA-PrPT delivers improved efficacy to minimize PrP^{Sc} burden in the cells.

3.4. Evidence for continuum of PrP^{Sc} formation in ScN2a cells cured by RNAi

Although it appeared that ScN2a cells stably transfected with pShRNA-PrPT were cured, our data did not exclude the possibility that a minimal level of PrP^{Sc} kept being propagated from residual PrP^C by PrP^{Sc} remained at a level below the conventional detection limits. To address the ability of cured ScN2a cells in triggering prion propagation, stable transfectants analyzed in Fig. 3D and E were maintained for extended periods of time. Although PrP^{Sc} accumulation in each clone was not found at the same level, some clones of cured ScN2a cells showed PrP^{Sc} accumulation after the prolonged culture under the prion-free conditions (Fig. 4A). Levels of PrP^{Sc} in these cell clones were comparable to the mixed cell population of ScN2a cells stably transfected with the control shRNA construct, pShRNA-PrPS. However, PrP^{Sc} in a certain cured clone (T#7) remained at an undetectable level (Fig. 4A).

To simulate propagation of prions included in cured ScN2a cells, if any, cell lysate of the clone T#7 showing the least PrP^{Sc} accumulation (Fig. 4A) was applied to PMCA, a cell-free prion propagation system (Ryou and Mays, 2008). When the lysate of T#7 clone of cured ScN2a cells was diluted as “seeds” in brain homogenate of

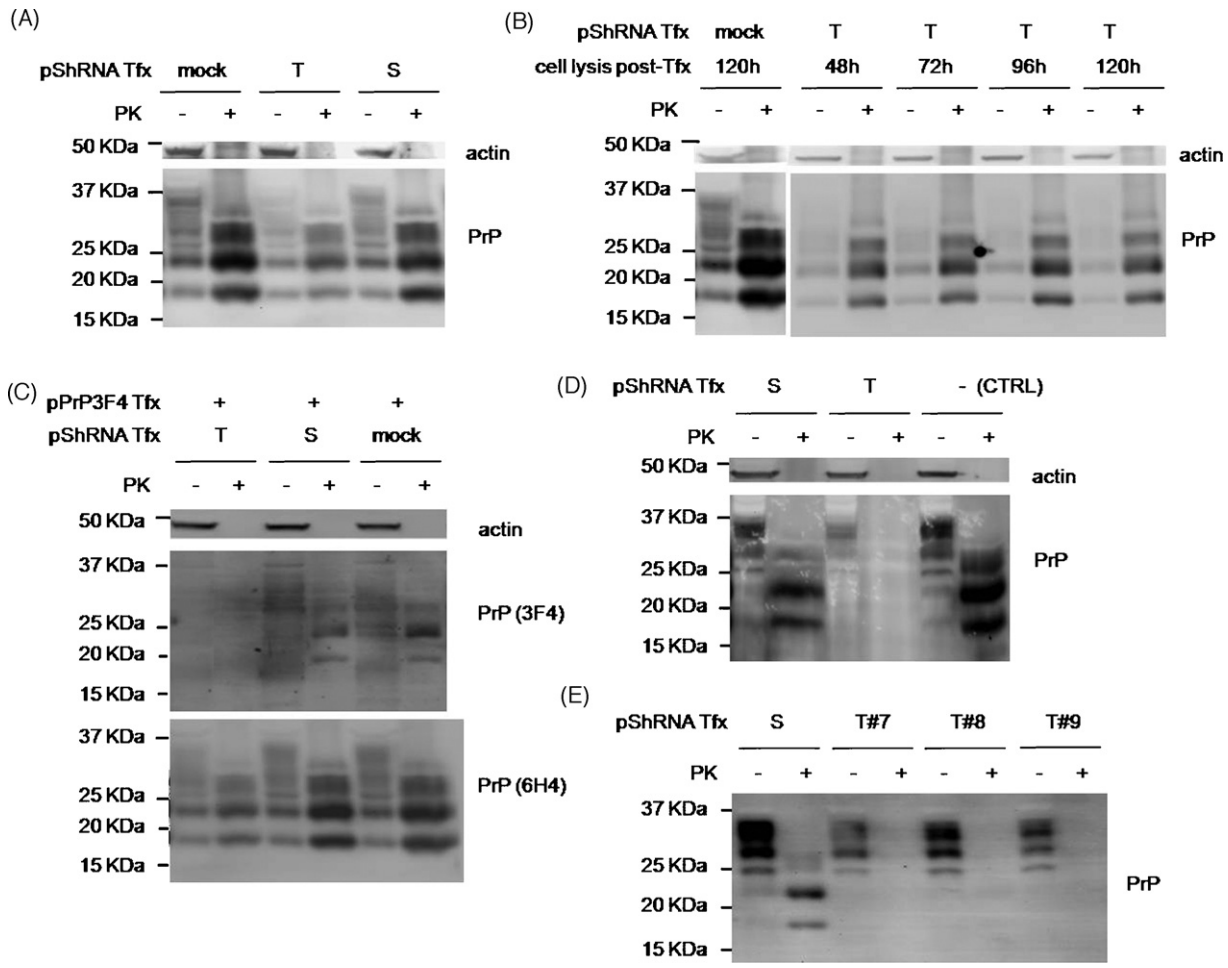

Fig. 3. Down-regulation of PrP^{C} and PrP^{Sc} in ScN2a cells transfected with shRNAs targeting *prnp*. ScN2a cells were transfected with pShRNA-PrPT (T) targeting *prnp* and pShRNA-PrPS (S) containing scrambled sequences. The mock transfection (Tfx) was performed with no pShRNA plasmid DNAs. (A) Measurement of endogenous PrP^{C} and PrP^{Sc} of transiently transfected ScN2a cells. The transfectants were analyzed 48 h post-transfection. (B) Changes in PrP^{C} and PrP^{Sc} levels during the time course (48–120 h post-transfection). (C) Measurement of newly generated PrP^{Sc}. The cells were co-transfected with pShRNA and pPrP3F4. The transfectants were analyzed 48 h post-transfection. The samples digested with and without proteinase K (PK) were divided and blotted with two different anti-PrP antibodies, 6H4 and 3F4. (D) Measurement of endogenous PrP^{C} and PrP^{Sc} of permanently transfected ScN2a cells. Stable transfectants were established by selection with hygromycin until mock transfected cells were removed completely. CTRL: ScN2a cell samples indicating the level of PrP^{Sc} in the cells before transfection. (E) The level of PrP^{C} and PrP^{Sc} in individual clones (T#7, 8, and 9) of stable transfectants with pShRNA-PrPT. The mixed population of stable transfectants with pShRNA-PrPS (S) served as control.

healthy Tg4112 mice for PMCA, minimal but obvious PrP^{Sc} propagation was observed (Fig. 4B). Cell lysate of the clone T#8 and 9 showing resurrected PrP^{Sc} accumulation (Fig. 4A) resulted in more PrP^{Sc} amplification than T#7 (Fig. 4B). However, this was less efficient than PrP^{Sc} amplification with untransfected ScN2a cells or mixed population of ScN2a cells stably transfected with pShRNA-PrPS, which include an excess amount of prions and support vigorous PrP^{Sc} propagation (Fig. 4B). To compare the effect of RNAi in eliminating PrP^{Sc} to previously reported chemical-based agents, "seeds" prepared from ScN2a cells cured by PAMAM G4.0 and quinacrine were utilized in PMCA. PrP^{Sc} was completely cleared in PAMAM G4.0- and quinacrine-cured cells (Fig. 4A). PMCA failed with "seeds" from those sources as it did with negative control "seeds" obtained from N2a cells (Fig. 4B). These results suggest that a minute amount of PrP^{Sc} was included in RNAi-cured cells and served as templates for nascent PrP^{Sc} formation. Thus, RNAi appears to be less efficient than PAMAM G4.0 and quinacrine in clearing PrP^{Sc} from the prion-infected cells. The reappearance (Fig. 4A) and amplification (Fig. 4B) of PrP^{Sc} in cured ScN2a cell clones suggest a continuum of PrP^{Sc} propagation within those cells and implicate potential prion transmission during forthcoming passages.

4. Discussion

Among many strategies, reduction of PrP^{C} levels is particularly attractive as a treatment for prion diseases since transgenic mice lacking PrP^{C} expression neither propagated prions nor developed pathology following inoculation with prions (Bueler et al., 1993; Sailer et al., 1994). Introduction of RNAi agents targeting *prnp* messages was effective in suppressing PrP^{C} expression and beneficial in treating prion diseases as demonstrated in recent reports (Pfeifer et al., 2006; White et al., 2008). In agreement with these studies, our investigation confirmed that RNAi approach knocked down PrP^{C} expression and inhibited PrP^{Sc} formation in cell culture models of prion diseases. We attempted to find an RNAi region that effectively silences PrP^{C} expression. Subsequently, we confirmed that expression of shRNA harboring this RNAi region in cultured neuroblastoma cells specifically knocked down expression of PrP gene transcripts and proteins. Application of such shRNA construct in prion-infected cells resulted in clearance of PrP^{Sc} in the cell population. Since reduced PrP^{C} expression by RNAi significantly decreases the level of an essential substrate required for prion propagation, our results support that this approach could be an efficient strategy to suppress prion propagation.

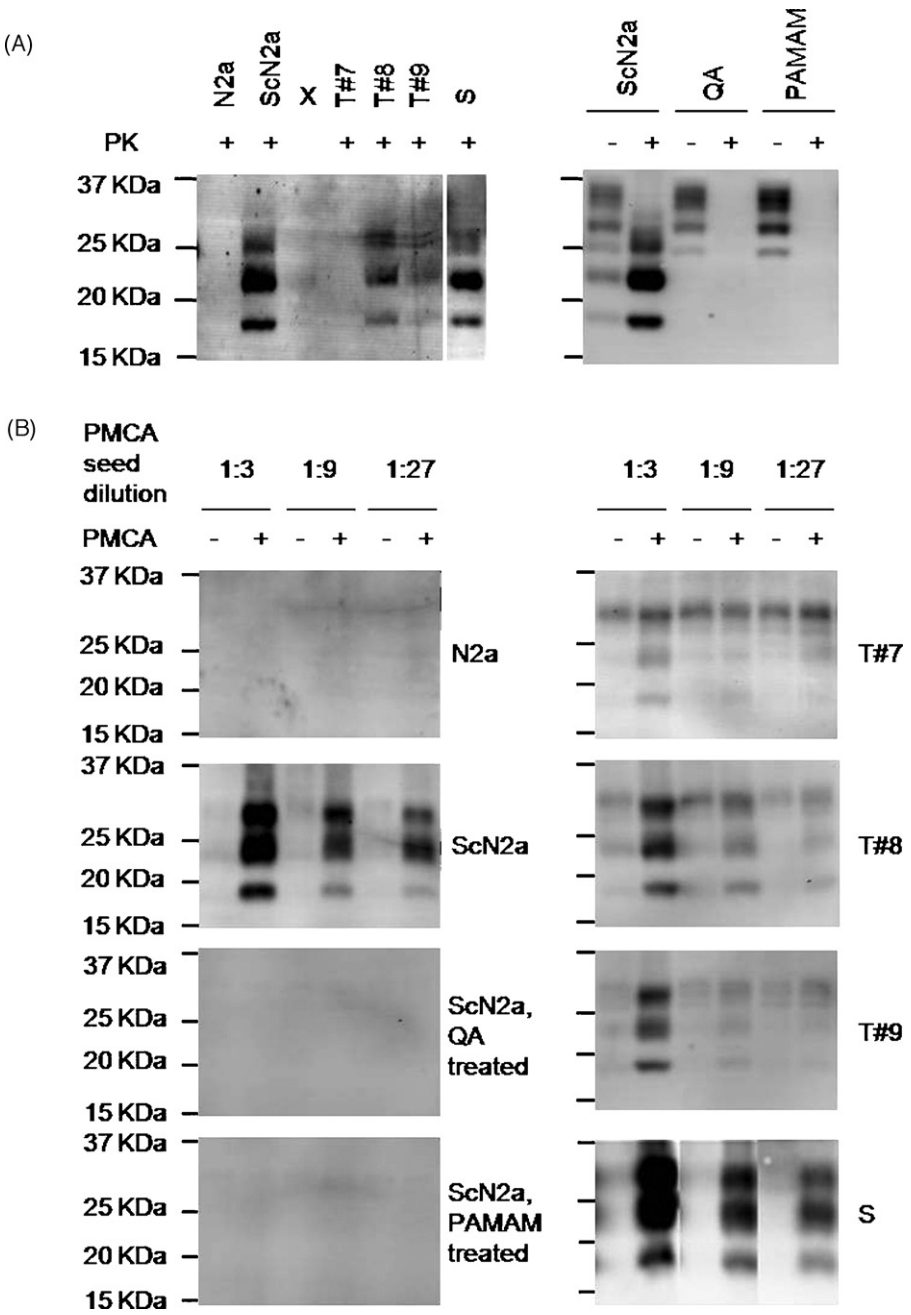

Fig. 4. PrP^{Sc} propagation in cured ScN2a cells. (A) Proteinase K (PK)-resistant PrP^{Sc} accumulation in the clones or mixed population of ScN2a cells either stably transfected with pShRNA constructs or cured by PAMAM G4.0 (PAMAM) and quinacrine (QA). At the end of 3-week selection, nine individual clones of stable transfectants with pShRNA-PrPT were obtained and separately maintained for additional 40 days. After the prolonged culture, three clones (T#7, 8, and 9) of cured cells were randomly chosen for analysis. The mixed population of stable transfectants with pShRNA-PrPS (S) served as control. ScN2a cells treated with 0.1 μM PAMAM and 0.6 μM QA for 6 days were also analyzed. X denotes an empty lane. (B) Protein misfolding cyclic amplification (PMCA) of PrP^{Sc} from cured cells. Lysates were prepared from N2a, ScN2a, S, T#7, 8, 9, PAMAM-treated ScN2a, and QA-treated ScN2a cells. PMCA was performed under conditions in which various cell lysates were diluted 1:3-, 1:9-, and 1:27-fold in brain homogenate of Tg4112 mice. The samples before (−) and after (+) PMCA were analyzed by Western blotting after PK digestion.

The RNAi approach used in our studies has a great potential in developing a versatile method to treat prion diseases. Although prion propagation is the central event for progress of all prion diseases (Ryou, 2007), the details in prion propagation may differ for individual prions, presumably due to prion strains and etiology. Thus, anti-prion agents targeting PrP^{Sc} or its formation could not be equally efficacious for all prion diseases because the conformation of PrP^{Sc} may differ in individual strains. In fact, some agents known to exhibit potent anti-prion activity demonstrate prion strain and source dependency (Adjou et al., 1997; Kawasaki et al., 2007; Supattapone et al., 2001). Unlike such agents, RNAi could be universally applicable to all types of prion diseases regardless of infecting prion strains or etiology of disease because RNAi targets PrP^{C}, the only substrate for prion conversion and the common substrate for all different prion strains.

Although our results verify that RNAi strategy is useful for future application to obtain cell culture models expressing PrP^{C} at a reduced level, the problems associated with intrinsic limitations of RNAi such as incomplete elimination of PrP^{C} could be critical when applying this approach to the generation of animal models resistant to prion diseases. In the best case scenario, animals

expressing the reduced level of PrP^C (Gallozzi et al., 2008; Golding et al., 2006) may not develop prion disease. It is possible, however, that those animals accumulate the undetectable level of PrP^{Sc} and remain as asymptomatic disease carriers, leaving a potential risk for spreading disease.

Despite the evidence shown in our studies, the current form of RNAi approach does not fit in immediate medical practice. Several hurdles such as stability, delivery, specificity, and unexpected toxic side effect of RNAi need to be overcome for successful application of RNAi technology to therapy in medicine. Our studies raise an additional concern that this approach should require improvement before being used in therapy for prion diseases. Since RNAi with a single shRNA construct was unable to completely deplete PrP^C, de novo propagation of PrP^{Sc} was possible in the hosts. To overcome this problem, gene silencing by multiple shRNA constructs that target different regions of *prnp* messages could be useful to achieve more favorable outcomes in treating the disease. For successful implementation in the treatment of human patients affected by prion diseases, it would be more realistic to use RNAi approach in attenuating the progress of disease by limited tissue-specific delivery of shRNA via viral vectors as suggested (White et al., 2008). Because serious damage in the brain has already occurred before clinical signs are apparent during the course of prion diseases, it is difficult to reverse the damage and cure the diseases. Therefore, in complement with RNAi approach, treatment with a combination of agents accelerating elimination of pre-formed PrP^{Sc} and/or those regenerating damaged cells is worthy of consideration. This may open a novel avenue in searching for an effective treatment for prion diseases.

The inability of RNAi to clear pre-existing PrP^{Sc} is considered a drawback of using this approach in therapy for prion diseases. In previous studies, RNAi was not completely successful in curing prion-infected animals (Pfeifer et al., 2006; White et al., 2008), presumably due to the incomplete elimination of PrP^{Sc} that allowed disease progression to continue. However, our observation that PrP^{Sc} forms de novo in RNAi-cured cells suggests a novel alternative for this phenomenon. We found that PrP^{Sc} formation continuously occurred in cured ScN2a cells where PrP^C expression was suppressed by shRNA and PrP^{Sc} was reduced to the undetectable levels. This implicates the possibility of disease development from RNAi-cured hosts. Such a condition has not been described and is distinguished from that caused by pre-existing PrP^{Sc}. Although it is possible to achieve the condition of low burden for pre-formed PrP^{Sc} by initiating RNAi treatment early enough, the disease may reappear because of continuous PrP^{Sc} propagation that is intrinsic to this approach, thus preventing therapeutic success.

In conclusion, our studies confirmed that RNAi was sufficient to substantially reduce the level of PrP^C and remove PrP^{Sc} from prion-infected cells, which suggests a potential for treatment of prion diseases. However, the continuum of PrP^{Sc} propagation in cured cells raises a concern on the utility of the strategy to treat prion diseases. Our data presented in this report provide direct evidence of the limitations associated with RNAi-based therapeutic approaches for prion diseases, which have been conceptually speculated but not experimentally assessed. The limitations must be taken into consideration before applying RNAi-based prevention and therapy to human and animal prion diseases.

Acknowledgements

The authors thank Dr. Glenn Telling (University of Kentucky) for his generous gift of Tg4112 mouse brains and technical consultation on PMCA, and Ms. Paula Thomason for editing this manuscript. This work was supported in part by funds from the Sanders-Brown Center on Aging and College of Medicine, University of Kentucky.

References

Adjou, K.T., Deslys, J.-P., Demaimay, R., Dormont, D., 1997. Probing the dynamics of prion diseases with amphotericin B. Trends Microbiol. 5, 27–31.
Belay, E.D., Schonberger, L.B., 2005. The public health impact of prion diseases. Annu. Rev. Public Health 26, 191–212.
Bueler, H., Aguzzi, A., Sailer, A., Greiner, R.-A., Autenried, P., Aguet, M., Weissmann, C., 1993. Mice devoid of PrP are resistant to scrapie. Cell 73, 1339–1347.
Campochiaro, P.A., 2006. Potential applications for RNAi to probe pathogenesis and develop new treatments for ocular disorders. Gene Ther. 13, 559–562.
Castilla, J., Saa, P., Hetz, C., Soto, C., 2005. In vitro generation of infectious scrapie prions. Cell 121, 195–206.
Daude, N., Marella, M., Chabry, J., 2003. Specific inhibition of pathological prion protein accumulation by small interfering RNAs. J. Cell Sci. 116, 2775–2779.
Davidson, B.L., Boudreau, R.L., 2007. RNA interference: a tool for querying nervous system function and an emerging therapy. Neuron 53, 781–788.
Gallozzi, M., Chapuis, J., Le Provost, F., Le Dur, A., Morgenthaler, C., Peyre, C., Daniel-Carlier, N., Pailhoux, E., Vilotte, M., Passet, B., Herzog, L., Beringue, V., Costa, J., Tixador, P., Tilly, G., Laude, H., Vilotte, J.-L., 2008. Prnp knockdown in transgenic mice using RNA interference. Transgenic Res. 17, 783–791.
Golding, M.C., Long, C.R., Carmell, M.A., Hannon, G.J., Westhusin, M.E., 2006. Suppression of prion protein in livestock by RNA interference. Proc. Natl. Acad. Sci. U.S.A. 103, 5285–5290.
Grimm, D., Kay, M.A., 2007. Combinatorial RNAi: a winning strategy for the race against evolving targets. Mol. Ther. 15, 878–888.
Hannon, G.J., 2002. RNA interference. Nature 418, 244–251.
Kawasaki, Y., Kawagoe, K., Chen, C.-j., Teruya, K., Sakasegawa, Y., Doh-ura, K., 2007. Orally administered amyloidophilic compound Is effective in prolonging the incubation periods of animals cerebrally infected with prion diseases in a prion strain-dependent manner. J. Virol. 81, 12889–12898.
Kim, Y., Song, J., Mays, C., Titlow, W., Yoon, D., Ryou, C., 2009. Changes in gene expression of kringle domain-containing proteins in murine brains and neuroblastoma cells infected by prions. Mol. Cell. Biochem. 328, 177–182.
Livak, K.J., Schmittgen, T.D., 2001. Analysis of relative gene expression data using real-time quantitative PCR and the $2^{-\Delta\Delta CT}$ method. Methods 25, 402–408.
Mays, C.E., Kang, H.-E., Kim, Y., Shim, S.H., Bang, J.-E., Woo, H.-J., Cho, Y.-H., Kim, J.-B., Ryou, C., 2008. CRBL cells: establishment, characterization and susceptibility to prion infection. Brain Res. 1208, 170–180.
Ohnishi, Y., Tamura, Y., Yoshida, M., Tokunaga, K., Hohjoh, H., 2008. Enhancement of allele discrimination by introduction of nucleotide mismatches into siRNA in allele-specific gene silencing by RNAi. PLoS ONE 3, e2248.
Paddison, P.J., Caudy, A.A., Hannon, G.J., 2002. Stable suppression of gene expression by RNAi in mammalian cells. Proc. Natl. Acad. Sci. U.S.A. 99, 1443–1448.
Paddison, P.J., Caudy, A.A., Sachidanandam, R., Hannon, G.J., 2004. Short hairpin activated gene silencing in mammalian cells. Methods Mol. Biol. 265, 85–100.
Pai, S.I., Lin, Y.Y., Macaes, B., Meneshian, A., Hung, C.F., Wu, T.C., 2006. Prospects of RNA interference therapy for cancer. Gene Ther. 13, 464–477.
Pfeifer, A., Eigenbrod, S., Al-Khadra, S., Hofmann, A., Mitteregger, G., Moser, M., Bertsch, U., Kretzschmar, H., 2006. Lentivector-mediated RNAi efficiently suppresses prion protein and prolongs survival of scrapie-infected mice. J. Clin. Invest. 116, 3204–3210.
Prusiner, S.B., 1982. Novel proteinaceous infectious particles cause scrapie. Science 216, 136–144.
Prusiner, S.B., 1998. Prions. Proc. Natl. Acad. Sci. U.S.A. 95, 13363–13383.
Ryou, C., 2007. Prions and prion diseases: fundamentals and mechanistic details. J. Microbiol. Biotechnol. 17, 1059–1070.
Ryou, C., Legname, G., Peretz, D., Craig, J.C., Baldwin, M.A., Prusiner, S.B., 2003. Differential inhibition of prion propagation by enantiomers of quinacrine. Lab. Invest. 83, 837–843.
Ryou, C., Mays, C.E., 2008. Prion propagation *in vitro*: are we there yet? Int. J. Med. Sci. 5, 347–353.
Saborio, G.P., Permanne, B., Soto, C., 2001. Sensitive detection of pathological prion protein by cyclic amplification of protein misfolding. Nature 411, 810–813.
Sailer, A., Bueler, H., Fischer, M., Aguzzi, A., Weissmann, C., 1994. No propagation of prions in mice devoid of PrP. Cell 77, 967–968.
Schmidt, F.R., 2005. About the nature of RNA interference. Appl. Microbiol. Biotechnol. 67, 429–435.
Scott, M.R., Kohler, R., Foster, D., Prusiner, S.B., 1992. Chimeric prion protein expression in cultured cells and transgenic mice. Protein Sci. 1, 986–997.
Scott, M.R.D., Butler, D.A., Bredesen, D.E., Walchli, M., Hsiao, K.K., Prusiner, S.B., 1988. Prion protein gene expression in cultured cells. Protein Eng. 2, 69–76.
Sontheimer, E.J., Carthew, R.W., 2005. Silence from within: endogenous siRNAs and miRNAs. Cell 122, 9–12.
Supattapone, S., Nguyen, H.-O.B., Cohen, F.E., Prusiner, S.B., Scott, M.R., 1999. Elimination of prions by branched polyamines and implications for therapeutics. Proc. Natl. Acad. Sci. U.S.A. 96, 14529–14534.
Supattapone, S., Wille, H., Uyechi, L., Safar, J., Tremblay, P., Szoka, F.C., Cohen, F.E., Prusiner, S.B., Scott, M.R., 2001. Branched polyamines cure prion-infected neuroblastoma cells. J. Virol. 75, 3453–3461.

Sutou, S., Kunishi, M., Kudo, T., Wongsrikeao, P., Miyagishi, M., Otoi, T., 2007. Knockdown of the bovine prion gene PRNP by RNA interference (RNAi) technology. BMC Biotechnol. 7, 44.

Tilly, G., Chapuis, J., Vilette, D., Laude, H., Vilotte, J.L., 2003. Efficient and specific down-regulation of prion protein expression by RNAi. Biochem. Biophys. Res. Commun. 305, 548–551.

White, M.D., Farmer, M., Mirabile, I., Brandner, S., Collinge, J., Mallucci, G.R., 2008. Single treatment with RNAi against prion protein rescues early neuronal dysfunction and prolongs survival in mice with prion disease. Proc. Natl. Acad. Sci. U.S.A. 105, 10238–10243.